Available online at www.sciencedirect.com
ScienceDirect
Journal of the European Ceramic Society 28 (2008) 1723–1730
www.elsevier.com/locate/jeurceramsoc

Young's modulus, density and phase composition of pressureless sintered self-sealed Si_3N_4/BN laminated structures

Z. Krstic *, V.D. Krstic

Centre for Manufacturing of Advanced Ceramics and Nanomaterials, Nicol Hall, Queen's University, Kingston, Ontario, Canada, K7L 3N6

Received 2 July 2007; received in revised form 1 November 2007; accepted 10 November 2007
Available online 14 February 2008

Abstract

New self-sealed Si_3N_4/BN-based laminated structures have been produced by a modified slip-casting process in a form of square cross-sections, varying the number of layers from 3 to 20 and their thickness from 70 to 1000 μm. The composition of Si_3N_4 layers consists of 7 wt.% Y_2O_3 (yttria) and 3 wt.% Al_2O_3 (alumina). The BN-based interfaces consist of 90 wt.% BN and 10 wt.% Si_3N_4 in SN − (BN + SN) laminates and 50 wt.% BN and 50 wt.% Al_3O_3 in SN − (BN + Al_2O_3) laminates.

Si_3N_4/BN-based laminates were densified by pressureless sintering at temperatures ranging from 1720 to 1820 °C for 1 h under static N_2 gas atmosphere.

The highest density was achieved with samples having 3 Si_3N_4 layers in SN − (BN + SN) laminates and 5 Si_3N_4 layers in SN − (BN + Al_2O_3) with an average layer thickness of 260 and 320 μm, respectively. Also, it was found that samples with the highest density exhibit the highest Young's modulus of 315 GPa in SN − (BN + SN) laminates and 320 GPa in SN + (BN + Al_2O_3) laminates.

The microstructure of the (BN + Al_2O_3) interface consists mainly of YAG phase with BN and Si_3N_4 as minor phases, while the microstructure of the (BN + SN) interface consists of BN and Si_3N_4 as major phases. A much higher level of porosity was observed in (BN + SN) interfaces than in (BN + Al_2O_3) interfaces.

Keywords: Laminates; Si_3N_4/BN; Self-sealed structure; Interface; Young's modulus

1. Introduction

Silicon nitride (Si_4N_4) is one of the most promising ceramic materials for structural application because of its good mechanical properties over a wide temperature range, good wear and corrosive resistance, low density and good thermal shock resistance. However, in spite of good properties, mentioned above, low reliability of this ceramic is considered to be the major limiting factor for wider use as a structural material.

One way of preventing catastrophic failure of monolithic ceramic's component is to design a structure with dense and strong layers (e.g. Si_3N_4, SiC, Al_2O_3, ZrO_2, etc.) separated by weak or porous layers of the same or different materials (Fig. 1).[1]

The weak interface serves to deflect the propagating crack and lower its stress intensity. Traditionally, the crack deflection is achieved by incorporating fibers into ceramic matrices.[2,3] However, the fabrication of fiber-reinforced ceramics is expensive and often unsuccessful in achieving required mechanical properties.[4] Another way of preventing catastrophic failure is the use of porous or intermittent interlayers, first studied by Atkins,[5] then followed by Clegg,[6] Zhang and Krstic[7] and Tu et al.[8]. One of the requirements for achieving high properties of the laminate is that the interface material must be chemically and physically compatible with the lamina, so that they can be both co-fired and used at an elevated temperature without any undesired reactions and delamination. This delamination, caused by internal stresses during sintering, can be prevented by incorporating porosity in the interlayers and by creating self-sealed structure. Lately, a pre-determined level of interlayer porosity to ensure crack deflection for the situation where residual stresses were not present, has been investigated and reported by Blanks et al.[9] and Davis et al.[10]. The process of adding Si_3N_4 fibers to

* Corresponding author.
E-mail address: Krsticz@post.queensu.ca (Z. Krstic).

0955-2219/$ – see front matter.
doi:10.1016/j.jeurceramsoc.2007.11.020

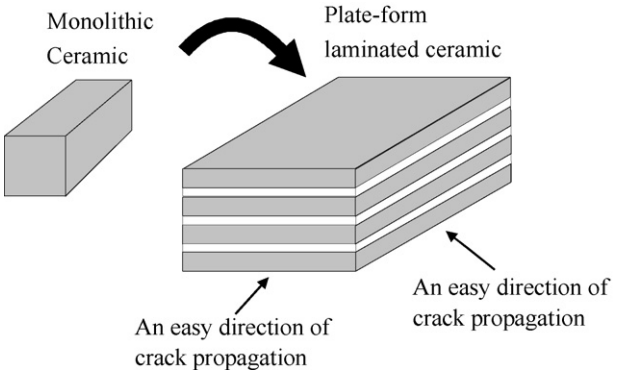

Fig. 1. Plate-form laminated ceramic with two directions of easy crack propagation.

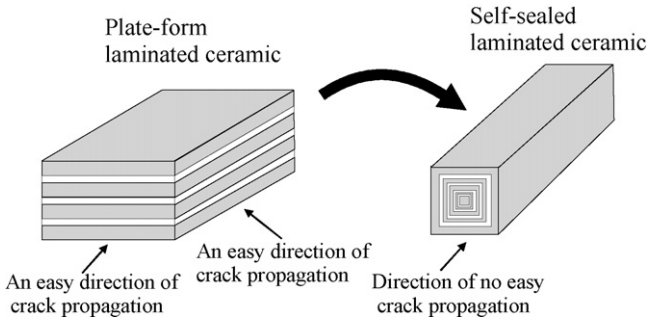

Fig. 2. New design concept involving transformation from plate-form to the self-sealed laminated structure.

Si_3N_4 powder to produce porous interlayers has been reported by Ohji et al.[11]. However, the major problem associated with a porous interlayer laminate is the difficulty in controlling the level of porosity and shape of the pores in the path of the growing interfacial crack.

In the last decade, efforts have been directed to developing a plate-form laminated ceramic composite with a weak interface such as SiC/graphite,[6] which exhibits fracture toughness as high as 14 MPa $m^{1/2}$.[7] Also, many investigators centered their attention on designing and processing plate-form laminated structures such as zirconia/zirconia (ZrO_2/ZrO_2),[12] alumina/monazite ($Al_2O_3/LaPO_4$),[13] silicon nitride/boron nitride (Si_3N_4/BN),[14] β-SiALON/Si_3N_4,[15] Al_2O_3/SiC,[4] Al_2O_3/ZrO_2,[16] mulite/Al_2O_3[17] and Al_2O_3/Al_2TiO_5.[18]

So far, the only fabrication techniques for laminates have been hot-pressing and hot-isostatic pressing. Recently, Wang et al.[19] produced planar laminates with apparent fracture toughness as high as 15.1 MPa $m^{1/2}$ by controlling composition and structure in Si_3N_4/BN laminates. Even higher fracture toughness of 28.1 MPa $m^{1/2}$ was obtained by adding secondary reinforcement such as SiC whiskers to the BN interface. Impressive increases in fracture strength and work of fracture of >600 MPa and ~8000 J/m^2, respectively, have been achieved by hot-pressing of Si_3N_4/BN laminates, as reported by Kovar et al.[20].

The major disadvantage of these plate-form laminates is that they possess two delamination directions of easy crack propagation which limit their wide application as structural components (Fig. 2). One possible solution to the intrinsic delamination problem associated with the plate-form ceramic laminates is to imitate natural materials, such as the ring structure of wood trunk in three-dimensions. In this paper, a new so called self-sealed structure decreases the potential delamination directions from two to zero when the structure of a laminate changes from a plate-form to a self-sealed rectangular structure (Fig. 2).[21,22]

Furthermore, self-sealed laminated structures can be effectively produced by employing traditional ceramic processing techniques such as modified slip casting, which allows varying the casting time, changing the composition and controlling the viscosity of the slurries in order to get different numbers of layers with different thicknesses.

This paper reports the results of a novel concept of the self-sealed Si_3N_4/BN laminated structure produced by slip-casting and pressureless sintering. The research is focused on the new structural design of laminates by creating concentric tree trunk structures of rectangular cross-section and to examine the effect of the number of layers and their chemical composition on Young's modulus, density and phase compositions of sintered laminates.

2. Experimental procedure

Commercially available, high purity α-Si_3N_4 powder (UBE E-10) was used as a starting material. Also, commercially available sub-micron size Al_2O_3 powder (A-16, Alcoa Chemical, Bauxite, USA) and high-purity sub-micron size Y_2O_3 powder (99.99%) (Alpha Aesar) were used as sintering additives. Hexagonal BN powder produced by Carborundum Company grade HPP-325 was used to create the weak interfaces.

Si_3N_4 water-based slurry was prepared by mixing 90 wt.% Si_3N_4, 7 wt.% Y_2O_3 and 3 wt.% Al_2O_3 with a solid-to-liquid ratio of 30/70 by volume. BN slurry was prepared by mixing BN and Al_2O_3, and BN and Si_3N_4 in a liquid consisting of ethyl alcohol and water with an ethyl alcohol-to-water ratio of 30/70. The BN interface consisted of 90 wt.% BN and 10 wt.% Si_3N_4 (SN − (BN + SN)) and 50 wt.% BN and 50 wt.% Al_2O_3 (SN − (BN + Al_2O_3)). Both BN slurries had a solid-to-liquid ratio of 5/95 by volume.

Si_3N_4/BN-based laminates were slip-cast alternately with Si_3N_4 layers and BN-based interfaces in plaster of Paris moulds with casting chambers of rectangular/square cross-sections of 8 mm × 8 mm and a length of ~60 mm (Fig. 3). All laminates were fabricated in such a way that the outside layer and core are Si_3N_4.

Pressureless sintering was carried out using a graphite resistance furnace (Vacuum Industries, Somerville, MA, USA) at temperatures ranging from 1740 to 1800 °C for 1 h under static N_2 gas atmosphere.

The densities of sintered Si_3N_4/BN laminates are given in terms of relative density, which is the ratio of the measured density of a sample to its theoretical density. The measured density was determined by the water displacement method.

Phase analysis was conducted on polished samples using an X-ray diffractometer (Model IGC-5, Rigaku Denki Co.

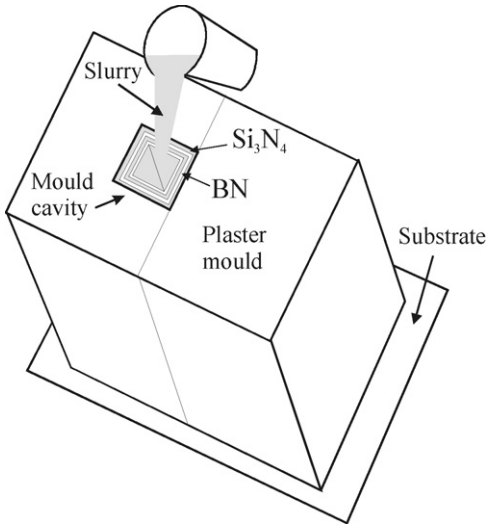

Fig. 3. Schematic view of slip-casting process.

Ltd., Japan), with Cu Kα radiation and a scanning rate of 2°/min.

The Young's modulus of the samples was measured using an impulse-excitation of vibration technique (Grindo-Sonic MK5, J.W. Lemmens, Inc. St. Louis, MO, USA) according to ASTM standards C 1259-94. This method covers a dynamic determination of the elastic properties of materials at ambient temperature.

3. Results and discussion

One of the objectives of this work was to design and fabricate laminated structures possessing no direction of easy crack propagation, termed self-sealed laminates. Fig. 4 shows the cross-sections of the cast rectangular forms. The structure is produced by slip-casting and pressureless sintering of alternate layers of Si_3N_4 and BN. As shown in Fig. 4, the structure consists of homogeneous Si_3N_4 layers (grey phase) separated by the uniform BN (white phase) interface. No delamination is observed during sintering and cooling to room temperature.

In these samples the largest thickness of a Si_3N_4 layer was approximately 1000 μm and the smallest was ~50 μm. The average thickness of the BN-based interface was approximately 12–15 μm. Due to the nature of the slip-casting process, the thickness of the previous Si_3N_4 layers determines the thickness of the next layer. As the layer thickness becomes larger the removal of the water through the wall of the green body becomes more difficult and, for a given casting time, the layer thickness becomes smaller and smaller.

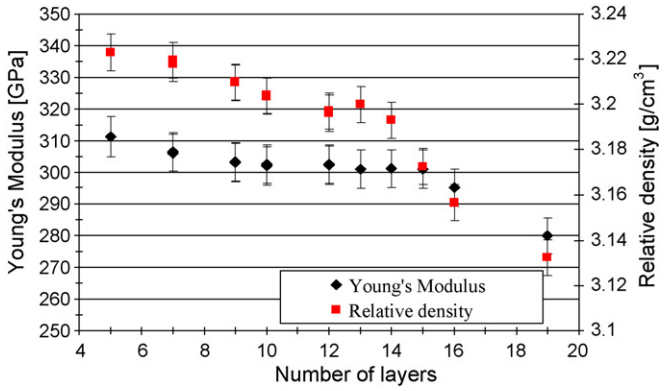

Fig. 5. Change of Young's modulus and relative density for samples containing 10 wt.% Si_3N_4 in the interface (SN – (BN + SN)).

The effect of the number of layers on sintered density (relative density) and elastic modulus (Young's modulus) is presented in Fig. 5 for laminates whose interface consists of 50 wt.% BN and 50 wt.% Al_2O_3 (SN – (BN + Al_2O_3)) and in Fig. 6 for laminates whose interface consists of 90 wt.% BN and 10 wt.% Si_3N_4 (SN – (BN + SN)). Both Figs. 5 and 6 show a decrease in relative density with the number of layers. This decrease in density is caused by the presence of an increased level of porosity in the interfacial layers and is also due to the addition of a lower density BN component. The highest density is found with samples containing the smallest number of layers and the lowest density was found with sample containing the largest number of layers. The effect of the number of layers and porosity on Young's modulus is also shown in Figs. 5 and 6. As mentioned before, an increase in the number of layers decreases the relative density, which in turn, lowers the Young's modulus of the structure. The decrease in density (or increase in porosity) has a strong

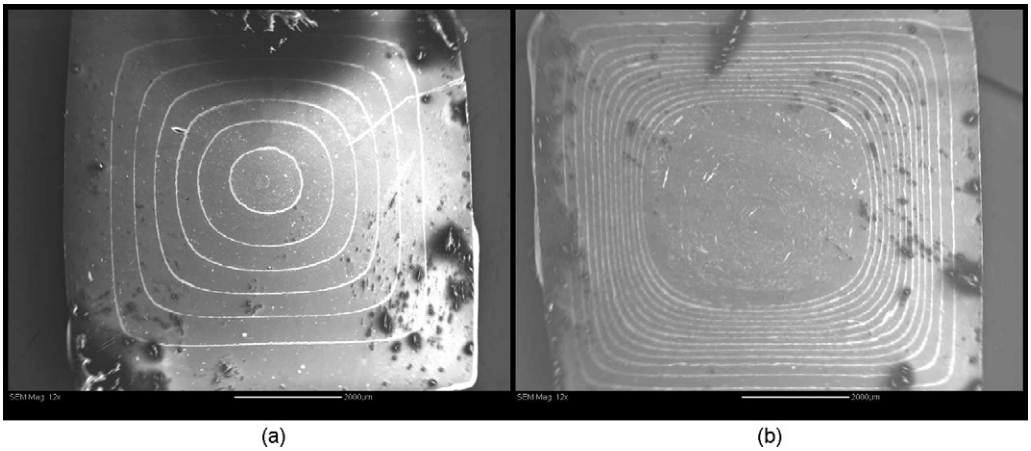

Fig. 4. SEM micrographs of self-sealed Si_3N_4/BN laminated structures with (a) 6 and (b) 13 Si_3N_4 layers.

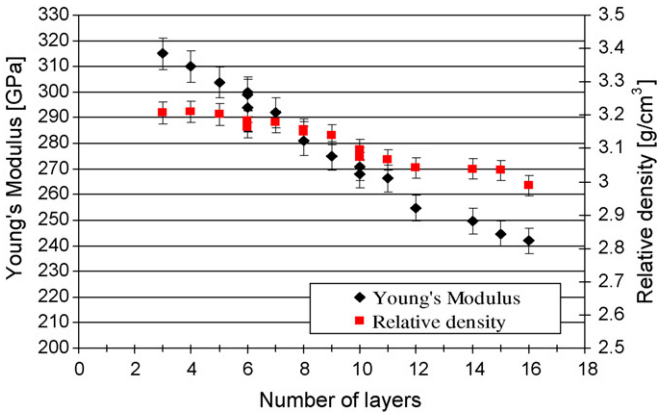

Fig. 6. Change of Young's modulus and relative density for samples which containing 50 wt.% BN + 50 wt.% Al_2O_3 the interface (SN − (BN + Al_2O_3)).

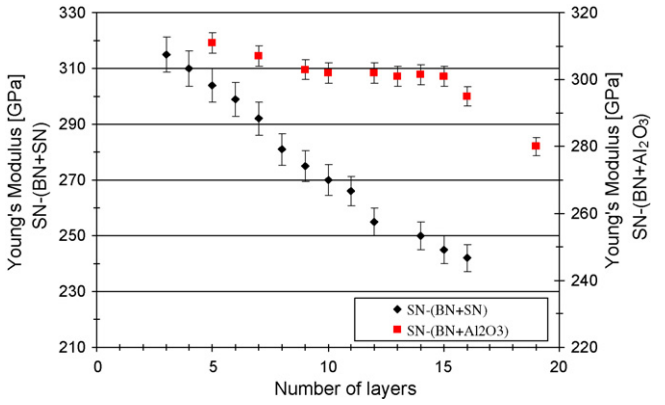

Fig. 7. Change of Young's modulus with the number of Si_3N_4 layers for interlayer containing 50 wt.% BN + 50 wt.% Al_2O_3 designated as SN − (BN + Al_2O_3) and 10 wt.% Si_3N_4 in BN designated as SN − (BN + SN).

effect on Young's modulus in that any small increase in porosity (equivalent to decrease in density) leads to a large decrease in Young's modulus.

Besides the porosity, BN is known to have low Young's modulus (33.86 GPa, in the *c* direction and 85.95 GPa in the *a* direction (at room temperature)) and this is the main reason for the reduction of Young's modulus of the whole system. Fig. 7 shows the change of Young's modulus with the number of layers for two different interlayer compositions. In one set of samples, the weak interfacial layer consists of 50 wt.% Al_2O_3 and 50 wt.% BN and the other consists of 10 wt.% Si_3N_4 and 90 wt.% BN. It can be seen from Fig. 7 that the laminated structure with interfaces containing 50 wt.% BN and 50 wt.% Al_2O_3 has a higher overall Young's modulus than the laminated structure with an interfaces containing 10 wt.% Si_3N_4 and 90 wt.% BN.

Much larger reduction in Young's modulus in SN − (BN + SN) laminates (Fig. 7) is caused by the apparent level of porosity in the interfacial layers. Careful examination of the interfaces in Fig. 8 revealed the presence of a much larger amount of porosity in layers containing BN and Si_3N_4.

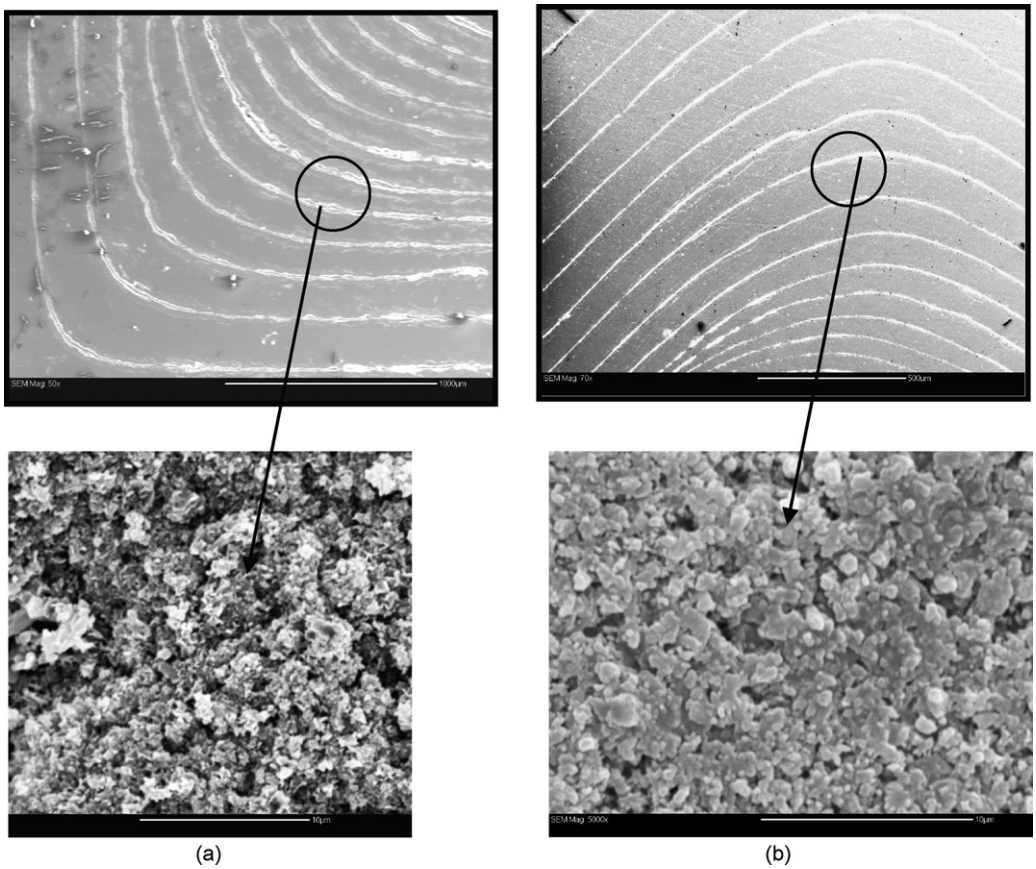

Fig. 8. Fracture surface of the interfaces (a) in SN − (BN + SN) and (b) in SN − (BN + Al_2O_3) laminated structures.

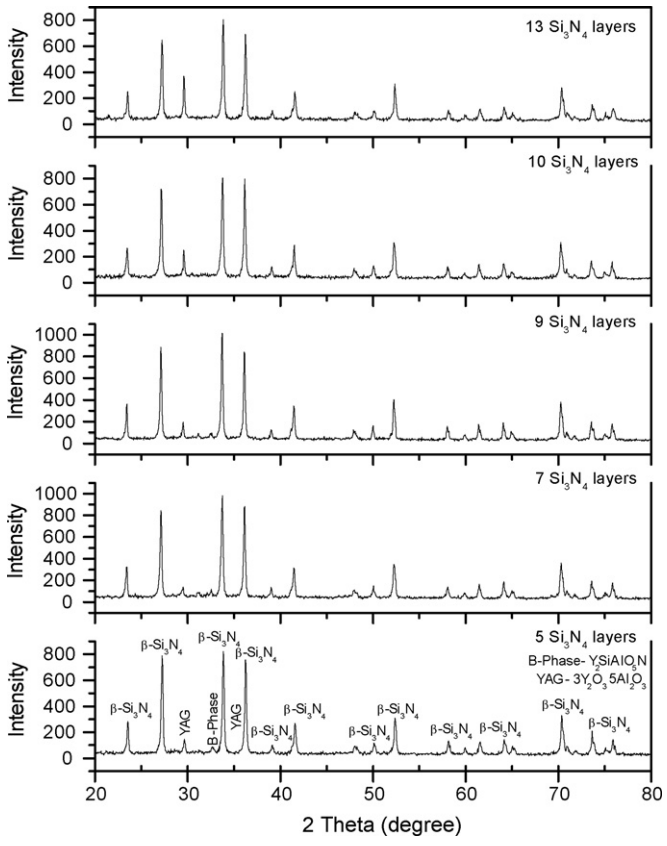

Fig. 9. X-ray diffraction patterns of SN − (BN + Al_2O_3) laminates with different number of layers sintered at 1760 °C.

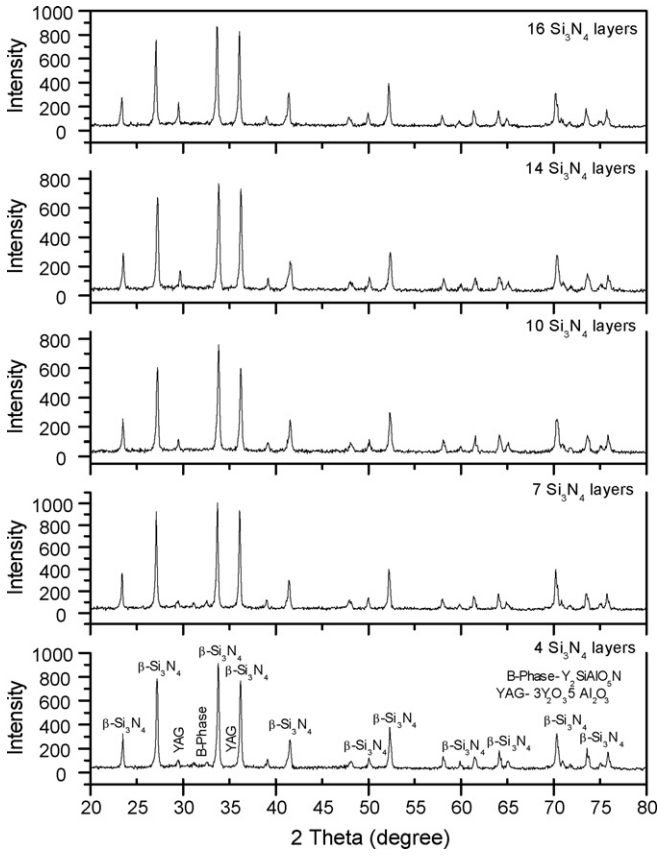

Fig. 10. X-ray diffraction patterns of SN − (BN + SN) laminates with different number of layers sintered at 1760 °C.

Laminates with interfacial layers containing 10 wt.% Si_3N_4 in BN appear to be less effective in promoting densification and results in a lower relative density and consequently a lower Young's modulus.

Figs. 9 and 10 show the X-ray patterns of cross-section of the Si_3N_4/BN-based laminates having different numbers of Si_3N_4 layers for compositions SN − (BN + Al_2O_3) and SN − (BN + SN), respectively. According to the X-ray data, the microstructure of the Si_3N_4 layers consists of a major β-Si_3N_4 phase and two minor phases, Y_2SiAlO_5N (B-phase) and $3Y_2O_35Al_2O_3$ (YAG). It can also be inferred from Figs. 9 and 10 that the amount of YAG phase increases continuously with the increase in the number of Si_3N_4 layers from 5 to 13 and 4 to 16. It can also be noticed that the increase in the amount of YAG phase takes place at the expense of B-phase, indicating that the Y_2SiAlO_5N (known as B-phase) decomposes to YAG and Si_3N_4.

It is also noticed that the entire amount of α-Si_3N_4 phase is transformed to β-Si_3N_4 phase in both compositions. It appears that the addition 10 wt.% of oxides (7 wt.% of Y_2O_3 and 3 wt.% of Al_2O_3) provides sufficient amount of liquid phase for complete α to β-Si_3N_4 phase transformation. The slow cooling rate of 10 °C/min. used in the present experiment was another favorable factor which contributed to complete decomposition of B-phase at temperatures between 1000 and 1100 °C. Another interesting finding of this work is the increase of YAG phase with an increase in the number of Si_3N_4 layers. It is found that a certain amount of Al_2O_3 present in the interface diffuses into the Si_3N_4 layers and some Y_2O_3 (after decomposition of B-phase) diffuses into BN-based interfacial layers. Finally, both Y_2O_3 and Al_2O_3 react with each other to form the YAG phase. An increase in the number of Si_3N_4 layers decreases the thickness of the layers and increases the number of the BN-based interfaces. The consequence of this is that the diffusion path for mass transport within the layers at the sintering temperature becomes shorter allowing easier diffusion and partitioning of Y_2O_3 and Al_2O_3 within the layers.

The X-ray diffraction patterns (Fig. 11) of the BN-based interfaces, when layers were broken/separated along the BN interface, show that, in addition to the presence of β-Si_3N_4 phase, three other phases are present: BN, B-phase and YAG. Again, the content of the YAG phase increases with an increase of the number of Si_3N_4 layers for up to 9 layers. When the number of layers is more than 9, the YAG phase becomes the major phase in the interfaces. This behaviour is consistent with the ability of the Y_2O_3 component to diffuse from the Si_3N_4 layer to the interfacial layer and react with Al_2O_3. As pointed out earlier, as the number of layers increases, their thickness decreases creating shorter diffusion paths for Y_2O_3 and faster reaction with Al_2O_3. The result of this is the larger amount of YAG phase formed in the interfacial layer. The decomposition of B-phase can be expressed by the

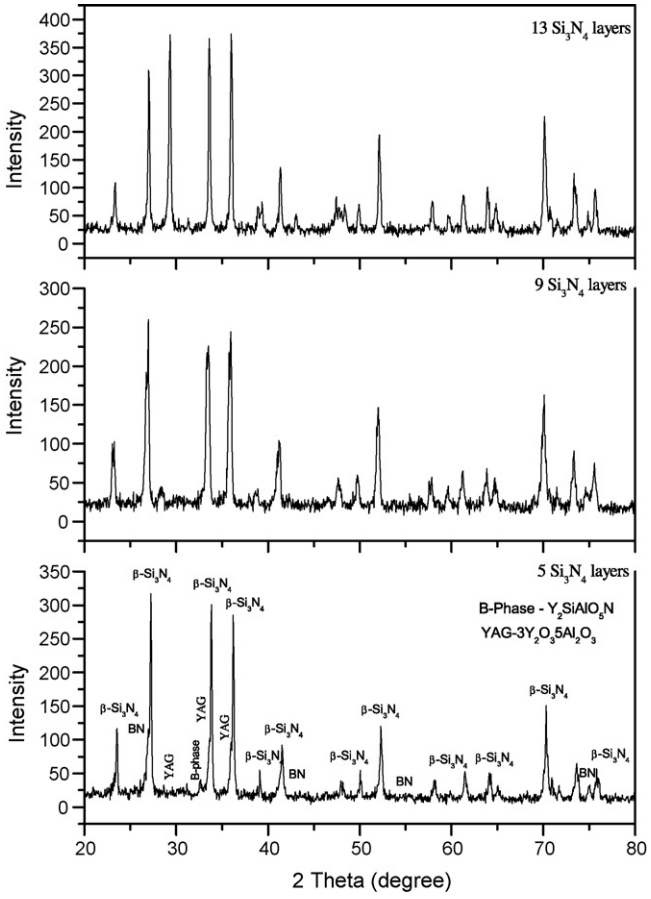

Fig. 11. X-ray diffraction patterns of BN interface with a different number of Si_3N_4 layers for SN – (BN + Al_2O_3) laminated structures sintered at 1760 °C.

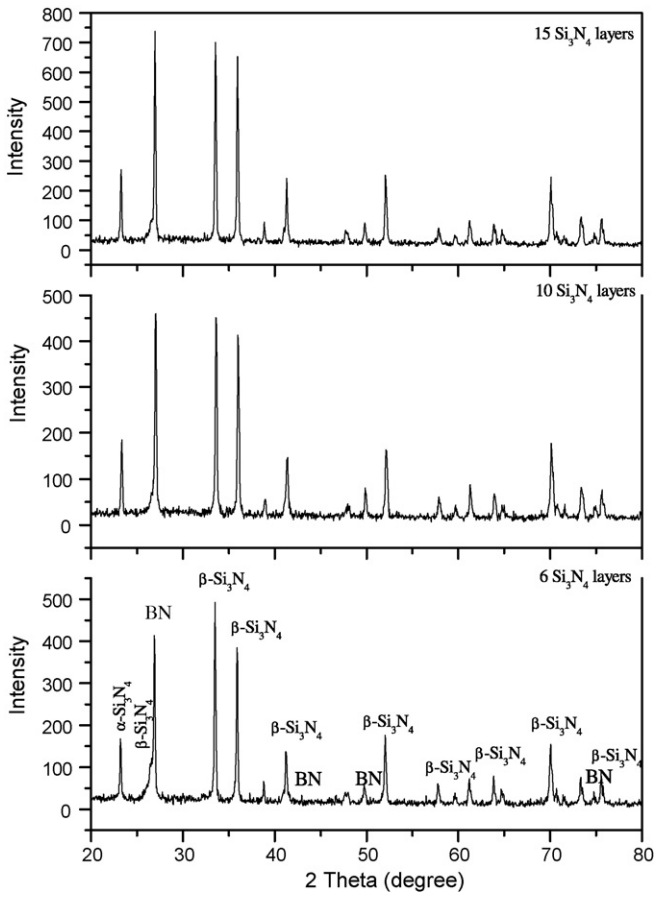

Fig. 12. X-ray diffraction patterns of BN-based interface with different number for Si_3N_4 layers of SN – (BN + SN) laminated structures sintered at 1760 °C.

reaction:

$$10Y_2SiAlO_5N \rightarrow 6Y_2O_3 + 3Y_2O_3{\cdot}5Al_2O_3 + Y_2Si_8O_6 + Si_2N_2O_2\uparrow + 4N_2\uparrow . \quad (1)$$

In turn, Y_2O_3 formed by Reaction (1) diffuses into the BN-based interface layer and reacts with Al_2O_3 to form YAG phase according to the reaction:

$$3Y_2O_3 + 5Al_2O_3 = 3Y_2O_3{\cdot}5Al_2O_3. \quad (2)$$

The support for this reaction mechanism is found in Fig. 11 which shows a continuous decrease of B-phase peak with the increase in the number of Si_3N_4 layers along with the increase of the intensity of X-ray peaks generated by the YAG phase.

Quite different X-ray diffraction patterns were produced in the laminates containing BN + Si_3N_4 interfacial layers (Fig. 12). Besides Si_3N_4 phase, only BN phase is detected and its amount increases with an increase of the number of Si_3N_4 layers. When the number of Si_3N_4 layers exceeds ~10, the BN phase becomes the major phase in the system. Expectedly, no YAG phase was observed in any of the laminates. Since the interface in the SN – (BN + SN) laminates consists of 90 wt.% BN and 10 wt.% Si_3N_4 there is no Y_2O_3 or Al_2O_3 present to form YAG phase. Although the X-ray diffraction did not detect the presence of YAG phase it should be emphasized that some small undetected amount of YAG may be present in the interface. The absence of YAG phase makes BN-based interfaces in SN – (BN + SN) laminated structures more porous than in SN – (BN + Al_2O_3) laminates. Considering that the BN phase has a low diffusivity, its sintering will be limited and it is expected that a much larger level of porosity will remain in these interfacial layers than in the BN + Al_2O_3 interfacial layers. Support for this statement is found from the results obtained from on Young's modulus measurement presented in Figs. 5–7 which show a much larger drop in Young's modulus for samples with BN + Si_3N_4 interfacial layers than for samples with BN + Al_2O_3 interfacial layers. The results are in line with prediction that a sharp reduction in Young's modulus is associated with porosity.

Initial mechanical properties measurements revealed a significant increase in apparent fracture toughness compared to the monolithic counterpart. The measurements also showed the effect of the Si_3N_4 layers number on the apparent fracture toughness, fracture strength and work of fracture (Table 1). The highest apparent fracture toughness of ~22 MPa $m^{1/2}$ and fracture strength of 470 MPa, respectively, were found for 7 Si_3N_4 layers in SN – (BN + Al_2O_3) laminates. Somewhat lower apparent fracture toughness of 19.5 MPa $m^{1/2}$ but higher fracture strength of 515 MPa were found for 4 Si_3N_4 layers in the SN – (BN + SN) laminates.

Table 1
The effect of the number of Si_3N_4 layers on mechanical properties of the self-sealed Si_3N_4/BN laminated structures

Number of Si_3N_4 layers	Materials					
	$SN-(BN+Al_2O_3)$			$SN-(BN+SN)$		
	Apparent fracture toughness (MPa $m^{1/2}$)	Strength (MPa)	Work of fracture (kJ/m^3)	Apparent fracture toughness (MPa $m^{1/2}$)	Strength (MPa)	Work of fracture (kJ/m^3)
3	–	–	–	17.2	337	150
4	10.4	100	100	19.5	515	225
5	11.2	290	125	16	412	279
7	22.3	470	200	16.3	375	300
9	16	367	230	13.2	300	320
11	12.8	322	150	13	220	246
13	10	310	140	–	–	–
Monolithic Si_3N_4	~9.2	~790	80	~9.2	~790	80

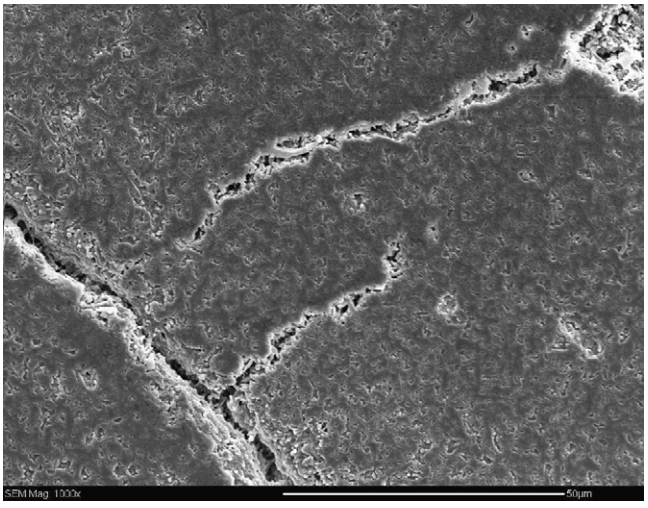

Fig. 13. A crack propagation through the Si_3N_4 layer and deflection at BN interface.

Fig. 14. Radial and axial direction of a crack propagation[22].

In the both laminates, there is an increase in the apparent fracture toughness and strength with number of Si_3N_4 layers followed by a decrease in the both by further increase in the layers numbers. It is believed that this increase of apparent fracture toughness and strength is attributed to the crack interaction (crack deflections) with the BN interphase. After deflection along the weak BN interphase (Fig. 13), crack propagation occurred in both radial and axial directions (Fig. 14). This led to an increase in apparent fracture toughness and fracture strength. Also, Table 1 reveals the effects of the number of Si_3N_4 layers on the work of fracture. The highest work of fracture of 230 and 320 kJ/m^3, respectively, are observed in $SN-(BN\text{-}Al_2O_3)$ and in $SN-(BN+SN)$ laminates.

4. Conclusion

Self-sealed Si_3N_4/BN-based laminated structures with square cross-section having different number of Si_3N_4 layers with different thickness have been fabricated for the first time using modified slip-casting method and densified by pressureless sintering process.

Neither delamination nor peeling during sintering or cooling from sintering temperature were observed in either $SN-(BN+Al_2O_3)$ or $SN-(BN+SN)$ laminated structures. The highest apparent density of over 3.22 g/cm^3 was achieved in $SN-(BN+Al_2O_3)$ with 5 Si_3N_4 layers, and the highest apparent density of 3.20 g/cm^3 was achieved in $SN-(BN+SN)$ laminates in samples having 3 Si_3N_4 layers. In both laminates, $SN-(BN+Al_2O_3)$ and $SN-(BN+SN)$, it was found that the samples with highest apparent density were also samples with highest Young's modulus with values of over 310 and 315 GPa, respectively.

The microstructure of Si_3N_4 layers in both laminates consists of β-Si_3N_4 phase, YAG phase and smaller amount of B-phase. The microstructure of the BN-based interface in $SN-(BN+Al_2O_3)$ laminates consists mainly of YAG phase with BN and Si_3N_4 as minor phases. Low level of porosity was observed in this interfaces. The microstructure of the BN-based interface in $SN-(BN+SN)$ laminates consists of BN and Si_3N_4 as major phases without the presence of YAG phase. A much

higher level of porosity was found in these interfaces than in $BN + Al_2O_3$ interface. The level of porosity in both BN-based interfaces is controlled by the amount of YAG phase present in the interface. The interface with higher content of YAG phase contains lower level porosity, as well as higher Young's modulus.

Due to the crack interaction with BN interface in radial and axial direction, very high apparent fracture toughness, strength and work of fracture are found in these laminates.

References

1. Clegg, W. J., Kandall, K., Alford, N. M., Birchall, D. and Button, T. W., A simple way to make tough ceramics. *Nature*, 1990, **347**, 455–457.
2. Kovar, D., King, B. H., Trice, R. W. and Halloran, J. W., Fibrous monolithic ceramics. *J. Am. Ceram. Soc.*, 1997, **80**, 2471–2487.
3. Koh, Y. H., Kim, H. W. and Kim, H. E., Mechanical properties of three-layered monolithic silicon nitride-fibrous silicon nitride/boron nitride monolith. *J. Am. Ceram. Soc.*, 2002, **85**, 2840–2842.
4. She, J., Inoe, T. and Ueno, K., Multilayer Al_2O_3/SiC ceramics with improved mechanical behavior. *J. Eur. Ceram. Soc.*, 2000, **20**, 1771–1775.
5. Atkins, A. G., Imparting strength and toughness to brittle composites. *Nature*, 1974, **252**, 116–118.
6. Clegg, W. J., The fracture and failure of laminar ceramic composites. *Acta Metall. Mater.*, 1992, **40**, 3085–3093.
7. Zhang, L. and Krstic, V. D., High toughness silicon carbide/graphite laminar composite by slip casting. *Theor. Appl. Fract. Mech.*, 1995, **24**, 13–19.
8. Tu, W. C., Lange, F. F. and Evans, A. G., Concept for a damage tolerant composite with "strong" interfaces. *J. Am. Ceram. Soc.*, 1996, **79**(2), 417–424.
9. Blanks, K. S., Kristofferson, A., Carlstorm, E. and Clegg, W. J., *J. Eur. Ceram. Soc.*, 1998, **18**, 1945–1951.
10. Davis, J. B., Kristofferson, A., Carlstorm, E. and Clegg, W. J., Fabrication and crack deflection in ceramic laminates with porous interlayers. *J. Am. Ceram. Soc.*, 2000, **83**, 2369–2374.
11. Ohji, T., Shigegaki, Y., Miyajima, T. and Kanzaki, S., Fracture resistance behavior of multilayered silicon nitride. *J. Am. Ceram. Soc.*, 1997, **80**, 991–994.
12. Sanchez-Herencia, A. J., Pascual, C., He, J. and Lange, F. F., ZrO_2/ZrO_2 layered composites for crack bifurcation. *J. Am. Ceram. Soc.*, 1999, **82**, 1512–1518.
13. Mawdsley, J., Kover, D. and Halloran, J. W., Fracture behavior of alumina/monazite multilayer laminates. *J. Am. Ceram. Soc.*, 2000, **83**, 802–808.
14. Liu, H. and Hsu, S. M., Fracture behavior of multilayer silicon nitride/boron nitride ceramics. *J. Am. Ceram. Soc.*, 1996, **79**, 2452–2457.
15. Shigegaki, Y., Brito, M. E., Hirao, K., Toriyama, M. and Kanzaki, S., β-SiALON-silicon nitride multilayered composites. *J. Am. Ceram. Soc.*, 1997, **80**, 2624–2628.
16. Plucknett, K. P., Caceres, C. H., Hughers, C. and Wilkinson, D. S., Processing of tape cast laminates prepared from fine alumina/zirconia powders. *J. Am. Ceram. Soc.*, 1994, **77**, 2145–2153.
17. Katsuki, H. and Hirata, Y., Coat of alumina sheet with needle-like mulite. *J. Ceram. Soc. Jpn.*, 1990, **98**, 1114–1119.
18. Russo, C. J., Harmer, M. P., Chan, M. H. and Miller, G. A., Design of laminated ceramic composites for improved strength and toughness. *J. Am. Ceram. Soc.*, 1992, **75**, 3396–3400.
19. Wang, C., Huang, Y., Zan, Q., Zou, L. and Cai, S., Control of composition and structure in laminated silicon nitride/boron nitride composites. *J. Am. Ceram. Soc.*, 2002, **85**, 2457–2461.
20. Kovar, D., Thouless, M. D. and Halloran, J. W., Crack deflection and propagation in layered silicon nitride/boron nitride ceramics. *J. Am. Ceram. Soc.*, 1998, **81**, 1004–1012.
21. Yu, Z. B. and Krstic, V. D., Fabrication and characterization of laminated SiC ceramics with self-sealed ring structure. *J. Mater. Sci.*, 2003, **38**, 4735–4738.
22. Yu, Z., Krstic, Z. and Krstic, V. D., Laminated Si_3N_4/SiC composites with self-sealed structure. *Key Eng. Mater.*, 2005, **280–283**, 1873–1876.